MCB
Journals.ASM.org

DLC1 Interaction with α-Catenin Stabilizes Adherens Junctions and Enhances DLC1 Antioncogenic Activity

Veenu Tripathi, Nicholas C. Popescu, and Drazen B. Zimonjic

Laboratory of Experimental Carcinogenesis, National Cancer Institute, National Institutes of Health, Bethesda, Maryland, USA

The *DLC1* (for deleted in liver cancer 1) tumor suppressor gene encodes a RhoGAP protein that inactivates Rho GTPases, which are implicated in regulation of the cytoskeleton and adherens junctions (AJs), a cell-cell adhesion protein complex associated with the actin cytoskeleton. Malignant transformation and tumor progression to metastasis are often associated with changes in cytoskeletal organization and cell-cell adhesion. Here we have established in human cells that the AJ-associated protein α-catenin is a new binding partner of DLC1. Their binding was mediated by the N-terminal amino acids 340 to 435 of DLC1 and the N-terminal amino acids 117 to 161 of α-catenin. These proteins colocalized in the cytosol and in the plasma membrane, where together they associated with E-cadherin and β-catenin, constitutive AJ proteins. Binding of DLC1 to α-catenin led to their accumulation at the plasma membrane and required DLC1 GAP activity. Knocking down α-catenin in DLC1-positive cells diminished DLC1 localization at the membrane. The DLC1–α-catenin complex reduced the Rho GTP level at the plasma membrane, increased E-cadherin's mobility, affected actin organization, and stabilized AJs. This process eventually contributed to a robust oncosuppressive effect of DLC1 in metastatic prostate carcinoma cells. Together, these results unravel a new mechanism through which DLC1 exerts its strong oncosuppressive function by positively influencing AJ stability.

Cancer initiation and progression constitute a multistep process, associated with both structural changes in certain genes and alterations in the dynamics and magnitude of their expression. Mutations and various chromosome rearrangements can invariably change the nature of the gene-encoded message; different molecular interactions and epigenetic modifications can modulate gene expression. Accumulation of genetic and epigenetic abnormalities results in the appearance of deviant cells refractory to normal homeostatic regulatory mechanisms and with a newly acquired capacity for unlimited, self-sufficient proliferation (6, 20).

Activation of oncogenes and/or inactivation of tumor suppressor genes (TSG) is often associated with a neoplastic phenotype. Over the past few years, the *DLC1* gene, encoding a Rho GTPase-activating protein (RhoGAP), has been established as a genuine TSG and increasingly considered a metastasis suppressor gene in various cancers. Aberrant upregulation of Rho GTPases is a major factor in the neoplastic process and tumor progression to metastasis (13). *DLC1* plays a key role in regulation of actin cytoskeleton and focal adhesions, in the process of cell migration and invasion, tumor cell dissemination, and metastasis, and in programmed cell death and neoangiogenesis (13, 16, 19, 26, 39, 49, 64, 69). *DLC1* has been shown to be one of the most frequently inactivated TSGs, predominantly by epigenetic modifications (13, 29, 30, 58, 60, 66). Restoration of *DLC1* expression in various carcinomas and in multiple myeloma cell lines results in suppression of proliferation, tumorigenicity, and metastasis, which is attributed to this gene's intrinsic ability to inactivate RhoA, RhoB, RhoC, and to a lesser degree Cdc42 (17, 21, 27, 55, 59, 68). However, several studies with DLC1 GAP mutants showed that DLC1 can also exert its antioncogenic activity through RhoGAP-independent mechanisms (21, 39). The presence of an N-terminal sterile α-motif (SAM), a serine-rich (SR) region, and a C-terminal steroidogenic acute regulatory protein-related lipid transfer (START) domain, in addition to the GAP domain, strongly points to DLC1's capacity to interact with a variety of proteins other than Rho GTPases (13). This prediction was validated by yeast two-hybrid screening, and a number of binding partners of DLC1 have been identified and examined in human cells. DLC1 interactions with various proteins negatively regulated, independently cooperated with, or enhanced the oncosuppressive effect of DLC1 (31, 39, 45, 61, 62, 63).

In this study, we identified α-catenin, an E-cadherin-associated protein, as another binding partner of DLC1 in human cells, characterized the nature of their interaction, and presented evidence for its biological significance. It is generally recognized that α-catenin acts as a molecular link between the actin cytoskeleton and the classical cadherin–β-catenin complex of cell-cell junction and facilitates the formation of radial actin cables (12, 41, 56), which are necessary for stabilization of AJs. Disruption of cadherin-mediated cell-cell adhesion is the key step in the progression of various types of human cancers (5, 22). Reduced levels of α-catenin and E-cadherin have been found in different human cancers, including highly malignant breast, stomach, ovarian, colon, and prostate cancers (25, 40, 57). The loss of α-catenin appears to correlate better with the tumor's metastatic potential than the loss of E-cadherin (47).

Here we show that by means of mutually recognized binding sites, DLC1 specifically interacts with α-catenin, they get associated to the plasma membrane, and through α-catenin DLC1 becomes connected with proteins of the AJ complex, E-cadherin and β-catenin. DLC1–α-catenin interaction regulates E-cadherin mobility, modulates the actin belt around AJs, and

Received 16 November 2011 **Returned for modification** 9 December 2011
Accepted 21 March 2012
Published ahead of print 2 April 2012
Address correspondence to Nicholas C. Popescu, popescun@mail.nih.gov.

doi:10.1128/MCB.06580-11

stabilizes E-cadherin-based cell-cell adhesion. This stabilization of AJs is seemingly responsible for a robust DLC1 onco-suppressive activity.

MATERIALS AND METHODS

Vector construction and adenovirus production. Adenoviruses encoding DLC1 cDNA or LacZ were prepared as previously described (17). To determine the region of DLC1 interacting with α-catenin, a series of vectors for expression of truncated fragments of DLC1 with an N-terminal V5 tag were constructed. Briefly, cDNAs corresponding to truncated fragments were subcloned into the pENTER/D-TOPO vector (Invitrogen, Carlsbad, CA), and cDNA inserts were transferred into the pcDNA3.1/nV5-DEST vector by means of the Gateway system using LR Clonase (Invitrogen, Carlsbad, CA). All constructs were confirmed by DNA sequencing. Adenovirus encoding α-catenin was purchased from Vector Biolabs (Philadelphia, PA). The pCMV-XL5 vector containing cDNA of α-catenin was purchased from Origene (Rockville, MD) and used in PCR for subcloning of α-catenin full-length and deletion constructs with glutathione *S*-transferase (GST) fusion. PCR products of full-length VH1 [VH1(1–906)], VH1(1–390), VH2(391–650), and VH3(651–906) were subcloned into pENTER/D-TOPO (Invitrogen, Carlsbad, CA) by using the Gateway system and transferred to the DEST-17 Gateway vector. A truncated DLC1(Δ340–435) construct was made by using a site-directed mutagenesis kit (Agilent Technologies, Santa Clara, CA). All primers used in the study are shown in Table 1.

Cell lines, culture conditions, and transfections. Human embryonic kidney (HEK293), liver adenocarcinoma (SK-Hep1), prostate cancer (PC-3, DU-145), and immortalized normal prostate (RWPE-1) cell lines were purchased from American Type Culture Collection (Rockville, MD). Cells were cultured in RPMI 1640 or Dulbecco's modified Eagle medium (DMEM) (Invitrogen, San Diego, CA) supplemented with heat-inactivated 10% fetal bovine serum (FBS). The prostate carcinoma (PCA) cell line C4-2-B2 was purchased from ViroMed Laboratories, Inc. (Minneapolis, MN) and was cultured in T medium supplemented with 10% FBS in a humidified CO_2 incubator at 37°C. For immunoprecipitation, cells were transiently transfected using Lipofectamine 2000 (Invitrogen, Carlsbad, CA) according to the manufacturer's instructions and incubated for 48 h before use. To suppress α-catenin and DLC1 for immunoprecipitation (HEK 293 cells) and fractionation (RWPE-1), cells were transfected with 160 nM appropriate antisense oligonucleotide or with scrambled control and were harvested after 48 h. Small interfering α-catenin RNA (si-α-catenin) was from Santa Cruz Biotechnology, Santa Cruz, CA, and small interfering DLC1 RNA (siDLC1) was from Invitrogen, Carlsbad, CA. For stable transfection of short hairpin RNA (shRNA) of α-catenin, four kinds of SureSilencing shRNA plasmid vectors containing a neomycin resistance gene (SA Biosciences, Frederick, MD) were transfected using Lipofectamine 2000, and medium containing 400 μg/ml neomycin was changed after 48 h. After 2 weeks, single colonies were picked up and expanded. For stable transfection of the DLC1(R718E), DLC1(Δ340-435), and DLC1(435-1091) constructs in C4-2-B2 cells, transfection was done as mentioned above and stable clones were selected using 400 μg/ml neomycin.

Southern blotting. Genomic DNA was isolated from the cell lines used in the study, and10 μg of DNA was restriction digested using EcoRI overnight at 37°C. DNA was resolved on an 0.8% agarose gel and transferred to a nylon membrane. A *DLC1* fragment (465 bp) was amplified with the primers DLC1-1F and DLC1-1R using the PCR DIG probe synthesis kit (Roche Applied Science, Indianapolis, IN). Membrane was hybridized overnight using a DIG Easy Hyb kit (Roche Applied Science, Indianapolis, IN). After washing, the membrane was probed with anti-digoxigenin (DIG) antibody and detected by the chemiluminescent alkaline phosphatase substrate disodium 3-(4-methoxyspiro{1,2-dioxetane-3,2′-(5′-chloro)tricyclo[3.3.1.1^{3,7}]decan}-4-yl)phenyl phosphate (CSPD) (Roche Applied Science, Indianapolis, IN).

Immunoprecipitation and Western blotting. Cells were transduced or transfected with various DLC1 or α-catenin deletion constructs and lysed with NP-40 lysis buffer (BioSource, Camarillo, CA) containing protease inhibitor cocktail (Sigma, St. Louis, MO). Centrifugation was done at 4°C for 20 min at 12,000 × *g* to clear the lysate from cellular debris. The protein level was determined by the bicinchoninic acid (BCA) protein assay. Anti-V5 (Invitrogen, Carlsbad, CA) or Anti-DLC1 (H260) polyclonal antibodies, anti-α-catenin monoclonal antibody (Santa Cruz Biotechnology, Santa Cruz, CA,), or anti-GST was added to precleared cell lysates, followed by incubation overnight at 4°C. Protein G-Sepharose slurry (Zymed Inc., San Francisco, CA) was added, with further incubation for 2 h. Immunoprecipitates were washed and loaded on 4 to 12% SDS-PAGE gels (Invitrogen, Carlsbad, CA), transferred to nitrocellulose membranes (Invitrogen, Carlsbad, CA), and subjected to Western blotting. Proteins were visualized with horseradish peroxidase (HRP)-conjugated secondary antibodies and chemiluminescent HRP substrate (Millipore, Billerica, MA). Antibodies used in this study were DLC1 monoclonal antibody (BD Transduction Laboratories, San Diego, CA), α-catenin, and β-catenin antibodies (Santa Cruz Biotechnology, Santa Cruz, CA), and E-cadherin and green fluorescent protein (GFP) antibodies (Abcam, Cambridge, MA).

Immunofluorescence analysis. Cells were fixed with 4.0% paraformaldehyde for 20 min, followed by permeabilization with 0.2% Triton-X for 5 min, and then subjected to staining. The following primary antibodies were used for staining: goat polyclonal DLC1, mouse monoclonal anti-E-cadherin, anti-α-catenin, and anti-β-catenin (Santa Cruz Biotechnology, Santa Cruz, CA). Secondary antibodies used were anti-mouse Alexa Fluor 488, anti-goat Alexa Fluor 568, and anti-mouse Alexa Fluor 650 (Molecular Probes, Carlsbad, CA). For confocal images, cells were examined with a Zeiss LSM 510 NLO confocal system (Carl Zeiss Inc., Thornwood, NY) with an Axiovert 200 M inverted microscope and operating with a 30-mW argon laser tuned to 488 nm, a 1-mW HeNe laser tuned to 543 nm, and a 1-mW HeNe laser tuned to 633 nm. Images were collected in Zeiss AIM software (v. 4.0) using a 63× Plan-Apochromat 1.4-numerical-aperture (NA) oil immersion objective and a multitrack configuration where the Alexa 488, Alexa 594, and Alexa 633 signals were sequentially collected in separate photomultiplier tubes (PMTs) with a band-pass (BP) 500- to 530-nm filter, BP 565- to 615-nm filter, and BP 650- to 710-nm filter after excitation with 488-, 543-, and 633-nm lasers, respectively. Zoom was set at 0.7, and images were 512 × 512 pixels with line averaging of 4.

Peptide pulldown. N-terminally biotin-labeled peptides were synthesized by Biomatik (Wilmington, DE) and dissolved in 0.1% acetic acid water to give a concentration of 2 mg/ml. Five micrograms peptide was taken and mixed in 50 μl of streptavidin beads for 1 h, and then HEK 293 extract transfected with full-length or DLC1(340–630) was added to the beads, followed by 4 h of incubation at 4°C. Washing was done four times with NP-40 lysis buffer for each 5 min (each). In samples, 10 μl of SDS loading dye was added, boiled for 5 min, and loaded on 4 to 12% SDS-PAGE gels, transferred to nitrocellulose membranes, and subjected to Western blotting with anti-V5 or anti-β-catenin antibody.

Preparation of subcellular fractions. C4-2-B2 cells were transduced with adenovirus-encoded LacZ (Ad-LacZ) or Ad-DLC1; PC-3 cells were transduced with Ad-LacZ and α-catenin or Ad-DLC1 and α-catenin. Ten-centimeter plates were chilled at 4°C and washed with ice cold PBS twice to remove all medium. Cells were then washed in buffer A (100 mM sucrose, 20 mM HEPES pH 7.4, 1.5 Mm $MgCl_2$, 1 mM EGTA, 1 mM EDTA, and 1 mM dithiothreitol [DTT]) and resuspended in 500 μl of buffer B (buffer A plus 5% Percoll, 0.01% digitonin, protease inhibitor cocktails, and 1 mM phenylmethylsulfonyl fluoride [PMSF]). After 15 min of incubation on ice, unbroken cells and nuclei were pelleted by centrifugation at 2,500 × *g* for 10 min. The supernatant was centrifuged at 15,000 × *g* for 15 min to pellet mitochondria. Then supernatant was further centrifuged at 100,000 × *g* for 1 h. The resultant supernatant and

TABLE 1 Primers used in this study

Primer	Direction, sequence	Vector
V5-DLC1 1-1091	Forward, 5′ CACCATGTGCAGAAAGAAGCCGGAC Reverse, 5′ CTATCACCTAGATTTGGTGTCTTTGGT	pcDNA3.1/nV5-DEST
V5-DLC1 1-630	Forward, 5′ CACCATGTGCAGAAAGAAGCCGGAC Reverse, 5′ CTAAACCTTGATCCTCTTCATGAACTTGGG	pcDNA3.1/nV5-DEST
V5-DLC1 340-630	Forward, 5′ CACCATGGAGGGCTTCGATCCT Reverse, 5′ CTAAACCTTGATCCTCTTCATGAACTTGGG	pcDNA3.1/nV5-DEST
V5-DLC1 340-847	Forward, 5′ CACCATGGAGGGCTTCGATCCT Reverse, 5′ CTAGAAAAGCTTCTTGCACACGGC	pcDNA3.1/nV5-DEST
V5-DLC1 630-847	Forward, 5′ CACCATGTCCAGACTACAAGGACC Reverse, 5′ CTAGAAAAGCTTCTTGCACACGGC	pcDNA3.1/nV5-DEST
V5-DLC1 540-847	Forward, 5′ CACCATGCTCCGAGATCCCGGA Reverse, 5′ CTAGAAAAGCTTCTTGCACACGGC	pcDNA3.1/nV5-DEST
V5-DLC1 340-435	Forward, 5′ CACCATGGAGGGCTTCGATCCT Reverse, 5′ CTA GCT CAT GGA GCT GGA AGA ATT	pcDNA3.1/nV5-DEST
V5-DLC1 435-530	Forward, 5′ CACC ATG AGC AGC CGC CTG AGC ATC TAC Reverse, 5′ CTA GCT CAT GGA GCT GGA AGA ATT	pcDNA3.1/nV5-DEST
V5-DLC1 530-630	Forward, 5′ CACC ATG GGC AAC TCC CTG AAT GAA CCG Reverse, 5′ CTA GCC TGT GCT GTC CAG GTC GCT	pcDNA3.1/nV5-DEST
V5-DLC1 435-1091	Forward, 5′ CACC ATG AGC AGC CGC CTG AGC ATC TAC Reverse, 5′ CTATCACCTAGATTTGGTGTCTTTGGT	pcDNA3.1/nV5-DEST
V5-DLC1 Δ 340-435	Forward, 5′GGCATGTACTTAGAGGAGCAGCCGCCTGAG Reverse, 5′CTCAGGCGGCTGCTCCTCTAAGTACATGCC	pcDNA3.1/nV5-DEST
GST-α-catenin 1-906	Forward, 5′CACCATGACTGCTGTCCATGCAGGCAAC Reverse, 5′ CTATTAGATGCTGTCCATAGCTTTGAA	pDEST 27
GST-α-catenin 1-290	Forward, 5′ CACCATGACTGCTGTCCATGCAGGCAAC Reverse, 5′CTAGTCCACAATGATTTGTTTGTCAAA	pDEST 27
GST-α-catenin 291-650	Forward, 5′CACCATGATTGTGGACCCCTTGAGCTTC Reverse, 5′CTAGACATCAAAATCTTCTGTCTCAAAGTC	pDEST 27
GST-α-catenin 651-906	Forward, 5′CACCTTTGATGTCAGAAGCAGGACG Reverse, 5′CTATTAGATGCTGTCCATAGCTTTGAA	pDEST 27
Southern blotting		
DLC1-1F	5′ CACAGGACAACCGTTGCCTCAG	
DLC1-1R	5′ CTCTTCAGGGTGTTGAGATGGA	
GAPDH-F	5′ GAAGGTGAAGGTCGGAGTCA	
GAPDH-R	5′ GAAGATGGTGATGGGATTTC	

pellet were designated the cytosolic and membrane fractions, respectively. Membrane pellet was washed twice with buffer A and then dissolved in an appropriate amount of buffer A with 1.0% Triton-X.

Fluorescence recovery after FRAP analysis. Fluorescence recovery after photobleaching (FRAP) analysis was done utilizing a laser-scanning confocal microscope (LSM 510 NLO; Carl Zeiss, Thornwood, NY). Cells were transfected with GFP–E-cadherin and were plated on chamber cover glass (LabTEK II; Nunc, Rochester, NY) after 24 h. E-cadherin at cell-cell junctions was observed with the pinhole set at 1. GFP–E-cadherin was excited with an 488-nm argon laser. A C-Apochromat 63×/1.2 water immersion objective was used with scan zoom set to 3, and line averaging was 2. Three prebleach images were captured; the iris field diaphragm was closed to its minimum diameter, and the light path was cleared of filters, allowing exposure of the selected region of interest (ROI) to 100% transmission for bleaching for no more than 20 s. FRAP time series movies were then commenced, with an Argon laser at 5% transmission, and images were captured for a total of 200 s for recovery. To see the DLC1 and α-catenin effect on junctional E-cadherin accumulation, GFP–E-cadherin-tagged C4-2-B2 cells and sh-α-catenin-transfected C4-2-B2 cells were transduced with Ad-LacZ or Ad-DLC1 and incubated for 48 h. To produce a FRAP recovery curve, raw data generated from LSM NLO software were transferred to an Excel sheet and first adjusted by background subtraction at each time point of bleached spot, corrected to a time-matched ROI that had not been photobleached, and then normalized to

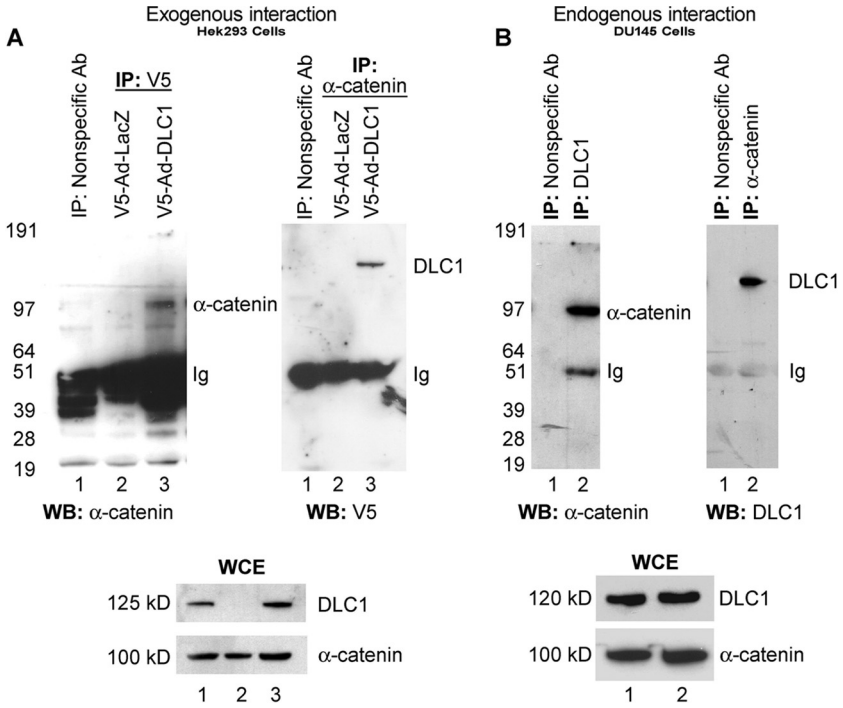

FIG 1 DLC1 interacts with α-catenin. (A) HEK 293 cells transduced with V5-Ad-LacZ (lane 2) or V5-Ad-DLC1 (lane 3) were lysed, immunoprecipitated with anti-V5 (left) or anti-α-catenin (right) antibodies (Ab), and analyzed by Western blotting (WB) with either anti-α-catenin or anti-DLC1 antibodies (lanes 2 and 3). The lower panel shows the whole-cell extract (WCE) of HEK 293 cells. (B) Immunoprecipitation of DU145 cell lysate with anti-DLC1 (left) or anti-α-catenin (right) antibodies and Western blotting with either anti-α-catenin or anti-DLC1 antibodies (lane 2). The lower panel shows the whole-cell extract of DU145 cells. Lane 1 shows immunoprecipitation with nonspecific antibody.

the background-subtracted prebleach image. To obtain mean curves, data from 10 images for each set of experiments were used.

Invasion assays. Cell invasion assays were performed using an 8-μm-pore-size BD Falcon FluoroBlok system (Becton, Dickinson, Franklin Lakes, NJ). Briefly, cells were transduced with Ad-DLC1 or Ad-LacZ or stably transfected with ShRNA of α-catenin and DLC1 truncated, and 2.5×10^4 cells/well were plated on ECMatrix gel-coated layered cell culture inserts. After 24 h, invaded cells were stained or quantified using calcein AM fluorescent dye (Becton, Dickinson, Franklin Lakes, NJ).

Colony formation in soft agar. A soft agar colony formation assay was performed as described previously (65) using a cell transformation detection assay kit (Chemicon, Temecula, CA). Cells were transduced with Ad-DLC1 or Ad-LacZ or stably transfected with shRNA of α-catenin and the DLC1(R18E) and DLC1 truncated mutants. These cells were suspended in 0.35% low-melting-point agarose, plated on a layer of 0.8% agarose in T-medium (5%) in six-well culture plates, and cultured at 37°C with 5% CO_2. After 4 weeks, colonies were stained and imaged. For quantitation, colonies were dissolved in cell quantification solution, and absorbance was measured at 490 nm.

Apoptosis analysis. C4-2-B2 cells were transduced with Ad-DLC1 or Ad-LacZ and stably transfected with shRNA of α-catenin; PC-3 cells were transduced with LacZ and Ad-α-catenin or Ad-DLC1 and Ad-α-catenin. Apoptosis analysis was done as described earlier (69). Samples were centrifuged and resuspended in fluorescein isothiocyanate (FITC)-labeled annexin V/propidium iodide (PI) according to the manufacturer's instructions (Chemicon, Temecula, CA). Apoptotic cells were analyzed by flow cytometry on a FACScan instrument (Becton, Dickinson, San Jose, CA).

Rhotekin binding assay for RhoA-GTP. To determine the effect of DLC1–α-catenin interaction on RhoA activation, we used the rhotekin binding assay for Rho GTP. C4-2-B2 cells were grown to confluence and then changed to serum-free medium for 24 h. Cells were lysed in 1× lysis buffer with inhibitor cocktail and 1 mM PMSF on ice for 5 min, and the lysates were centrifuged at 13,000 × *g* at 4°C for 3 min. One aliquot of lysate was analyzed for total protein content, and another aliquot was analyzed by Western blotting (normalized for total protein), to compare total RhoA content between samples. The remainder of the cell lysates was used for the RhoA activation assay as instructed by the manufacturer (Cell Biolabs, San Diego, CA). Rhotekin beads were incubated with cell lysates for 4 h and were washed thoroughly with washing buffer, and proteins attached to rhotekin were separated by SDS-PAGE in 12% acrylamide gels (100 V for 2 h). RhoA was detected with anti-RhoA primary antibodies (Abcam, Cambridge, MA).

RESULTS

DLC1 forms a protein complex with α-catenin. To confirm the interaction between DLC1 and α-catenin *in vitro*, human HEK293 cells ($DLC1^-/\alpha\text{-catenin}^+$) were transduced with V5-tagged adenovirus containing DLC1 (Ad-DLC1) and coimmunoprecipitated with anti-V5 or anti-α-catenin antibodies, and the interaction with α-catenin was detected by immunoblotting (Fig. 1A). To verify this interaction endogenously, protein extract from human PCA DU145 cell ($DLC1^+/\alpha\text{-catenin}^+$) was either immunoprecipitated with anti-DLC1 antibody and immunoblotted for α-catenin or immunoprecipitated with α-catenin antibody and immunoblotted for DLC1 (Fig. 1B). Coimmunoprecipitation of DLC1 with α-catenin by both experimental approaches showed that DLC1 forms an endogenous protein complex with α-catenin (Fig. 1B). To further verify this finding, we used ELISA; lysates of PC-3 ($DLC1^-/\alpha\text{-catenin}^-$) cells transduced with Ad-LacZ or Ad-DLC1 and Ad-α-catenin were added to 96-well plates previously coated with anti-α-catenin antibody, and after washing, bound complex was probed with anti-DLC1 antibody. Positive signal was

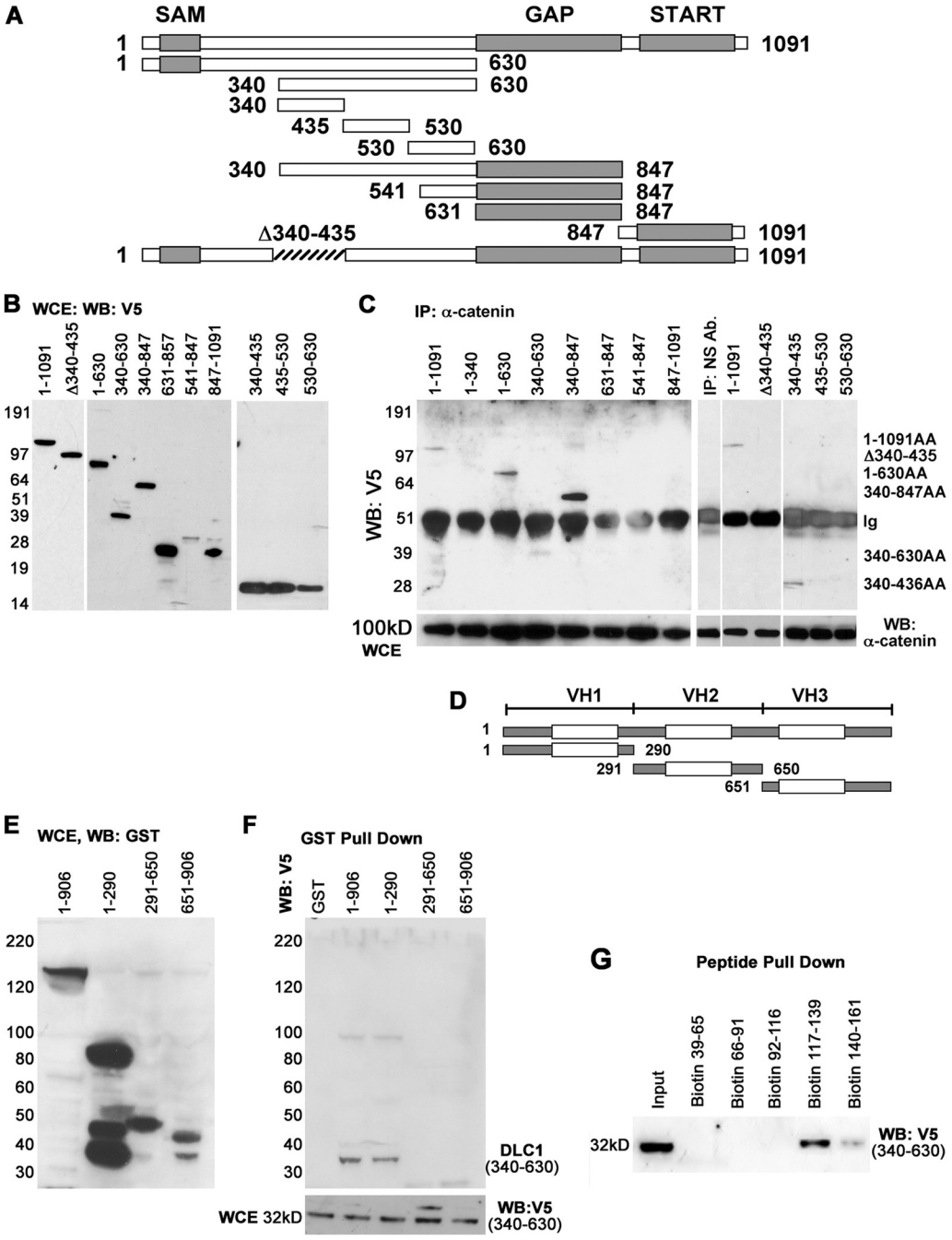

FIG 2 Identification of regions of DLC1 and of α-catenin responsible for interaction. (A) Schematic representation of V5-tagged DLC1 deletion constructs. (B) Expression of V5-tagged DLC1 deletion constructs in HEK 293 cells. (C) Probing of α-catenin-bound V5-tagged DLC1 deletion constructs with anti-α-catenin antibody shows that the DLC1 aa 340 to 435 region interacts with α-catenin. (D) Schematic representation of GST-tagged α-catenin deletion constructs. (E) Expression of α-catenin deletion constructs in HEK293 cells as detected by anti-GST antibody. (F) GST-tagged α-catenin deletion constructs were transfected into HEK 293 cells, and whole-cell extracts were pulled down with glutathione-Sepharose and probed with anti-V5 antibody to confirm that α-catenin's aa 1 to 290 region interacts with the aa 340 to 630 region of DLC1. (G) Streptavidin bead-based peptide pulldown of α-catenin's various biotin-labeled peptides (39–161 region) with cell extract of HEK 293 cells transduced with Ad-DLC1(340–630) and Western blotted with anti-V5 antibody.

observed only in wells containing lysates expressing both DLC1 and α-catenin, thus corroborating interaction between the two proteins (data not shown but available on request).

DLC1 aa 340 to 435 region interacts with α-catenin 117 to 161 region. Once we established binding between DLC1 and α-catenin, we sought to identify and characterize specific regions in their respective sequences that enable such interaction. For that, we used a V5-tagged vector to prepare a series of DLC1 deletion constructs (Fig. 2A), which were transfected in HEK293 cells, and we verified their expression by Western blotting (Fig. 2B, left). The ability of each expressed DLC1 protein variant to interact with α-catenin was tested by immunoprecipitation. Subsequent West-

ern blot analysis showed that of all the DLC1 variants, only those that contained the amino acid (aa) 340 to 630 segment of the DLC1 serine-rich region, between the SAM and GAP domains, were able to bind α-catenin (Fig. 2C, left).

More specifically, as demonstrated by use of even more detailed deletion constructs, 340–435, 435–530, and 530–630 (Fig. 2B and C, right), the site that carries out binding to α-catenin spans between amino acids 340 and 435 of the DLC1 protein. To further test the specificity of this site, we used a truncated (Δ340–435) V5 fusion construct of DLC1 (Fig. 2B, lane Δ340-435) and found that the Δ340–435 construct failed to bind α-catenin because of a lack of a critical 340 to 435 region (Fig. 2C, lane Δ340-435).

The same strategy was used to identify the site in the α-catenin amino acid sequence responsible for binding to DLC1. We created three GST-tagged deletion constructs (1–290, 291–650, and 651–906) of α-catenin, representative of its vinculin homology regions 1, 2, and 3 (VH1, VH2, and VH3), respectively (Fig. 2D), and verified their expression (Fig. 2E). After transfecting HEK293 cells with GST–α-catenin constructs, together with the V5-DLC1 340–630 construct, a GST pulldown assay showed that only the 1 to 291 region (VH1) of α-catenin interacted with the respective DLC1 340 to 630 site (Fig. 2F).

This VH1 region was further examined by a peptide pulldown assay using streptavidin beads and several biotin-labeled synthetic peptides spanning amino acids 39 to 65, 66 to 91, 92 to 116, 117 to 139, and 140 to 161 of the VH1 region of α-catenin. Results (Fig. 2G) showed that two segments within the α-catenin VH1 region bound to DLC1(340–630), namely, the 117 to 139 (DPCSSVKR GNMVRAARALLSAVTRLLI) and 140 to 161 (LADMADVYKLL VQLKVVEDGI) segments. It is worth noticing that interaction between DLC1 and α-catenin appears to be highly specific; vinculin, although an α-catenin-like protein, failed to bind to DLC1 (data not shown but available on request).

DLC1 interacts with AJ protein complex through α-catenin. To examine if DLC1 interacts with the AJ protein complex, HEK293 cells were transduced with V5-tagged Ad-DLC1 or LacZ and immunoprecipitated with anti-V5 antibody. The resulting immunopellet was Western blotted with anti-α-catenin, anti-β-catenin, and anti-E-cadherin antibodies, and the results (Fig. 3A) showed that DLC1 indeed associated with α-catenin, β-catenin, and E-cadherin, as predicted. However, this association was abrogated when the expression of α-catenin in HEK293 cells was suppressed by small interfering RNA (siRNA). To further validate these results, LacZ- or DLC1-transduced HEK293 cells were transfected with GFP–E-cadherin, and the respective lysates were immunoprecipitated with anti-GFP antibody (Fig. 3C). Subsequent Western blotting of the resulting immunopellets revealed association of GFP–E-cadherin with DLC1, α-catenin, and β-catenin. Yet again, suppression of α-catenin by siRNA resulted in abolition of GFP–E-cadherin/DLC1 grouping (Fig. 3C). Whole-cell extract showing protein input is presented in Fig. 3B. To confirm the association of DLC1 with AJs in cancer cells *in vitro*, a liver cancer line (SKHep1, $DLC1^{+}$/$\alpha\text{-catenin}^{+}$) and two PCA cell lines, C4-2-B2 ($DLC1^{-}$/$\alpha\text{-catenin}^{+}$) and PC-3 ($DLC1^{-}$/$\alpha\text{-catenin}^{-}$), were selected and transduced with Ad-DLC1. Before Ad-mediated transduction, both C4-2-B2 and PC3 were confirmed negative for DLC1 protein expression, although for different reasons: PC3 due to genomic deletion of *DLC1* loci and C4-2-B2 because of epigenetic silencing of the one remaining *DLC1* locus (Fig. 3 D and E). Also, comparison of DLC1 expression in C4-2-B2 and PC-3 cells transduced with Ad-DLC1 (multiplicity of infection [MOI] of 50), with intrinsic DLC1 expression in the RWPE-1 cell line, derived from normal prostate epithelium and used as a control in other studies (48), clearly established that that C4-2-B2 and PC-3 manifested the same level of DLC1 expression as the controls (Fig. 3F). Subsequently, both liver and prostate cells were lysed, and their extracts were immunoprecipitated with anti-DLC1 antibody.

Consistent with previous observations, in all cell lines the association of DLC1 with either E-cadherin or β-catenin occurred only in the presence of α-catenin (Fig. 3G). Immunoprecipitation of extracts with anti-E-cadherin antibody resulted in the same outcome (Fig. 3I), i.e., E-cadherin associated with DLC1 only in the presence of α-catenin, thus proving conclusively that DLC1/α-catenin interaction is causal for further DLC1 affiliation with other members of the AJ protein complex. Whole-cell extract showing protein input is presented in Fig. 3H.

Our results reveal that DLC1, β-catenin, and α-catenin are parts of a protein complex (Fig. 3A and G). To learn the nature of interactions in the complex, LacZ- or DLC1-tranduced HEK293 cells were transfected with GST alone or GST–α-catenin, the respective extracts were immunoprecipitated with anti-GST antibody, and resulting immunopellets were probed with anti-DLC1 or anti-β-catenin antibodies. The outcome showed that α-catenin interacted with both β-catenin and DLC1, but binding with β-catenin was more pronounced in the presence of DLC1 (Fig. 4A). Whole-cell extract showing input is presented in Fig. 4B. A peptide pulldown assay further demonstrated that while DLC1 shows a propensity to bind either the aa 117 to 139 or 140 to 161 region (Fig. 2G and 4C), β-catenin binds exclusively to α-catenin's 117 to 139 site (Fig. 4C). Given that the amount of β-catenin associated with α-catenin is larger in the presence of DLC1, it appears as if β-catenin's capacity for binding α-catenin is positively biased toward the α-catenin/DLC1 complex or that the bond established with the complex is either somewhat stronger or more stable. Confocal immunofluorescence analysis showed that full-length DLC1 colocalized with α-catenin both in the cytoplasm and at AJs, whereas its colocalization with E-cadherin and β-catenin occurred exclusively at AJs (Fig. 4D).

DLC1 and α-catenin interaction promotes accumulation of both proteins at the plasma membrane. Interaction of DLC1 with α-catenin not only provides DLC1 with access to AJs but also affects α-catenin in a very specific way. The PCA cell line C4-2-B2 lacks DLC1 but expresses a relatively high level of α-catenin, localized mostly to the cytoplasm. In contrast, another PCA cell line, PC-3, lacks both DLC1 and α-catenin. When PC-3 cells were transduced with Ad-α-catenin, the expressed protein localized throughout the cell, resembling its distribution in C4-2B2 cells. Interestingly, when C4-2-B2 cells were transduced with DLC1 and PC-3 cells were cotransduced with α-catenin and DLC1, and the latter was expressed up to the levels present in DLC1-positive prostate epithelial cells, and intracellular distribution of α-catenin in both cell lines abruptly changed: it diminished or completely disappeared from the cytoplasm but appeared in great quantity, or exclusively, at cellular membranes (Fig. 5A). Western blotting of cytosolic and membrane fractions of C4-2-B2 and PC-3 cells transduced with Ad-DLC1 or Ad-DLC1 and Ad-α-catenin, respectively, confirmed that in both cells lines expression of DLC1 causes significant relocation of α-catenin from the cytosol to the

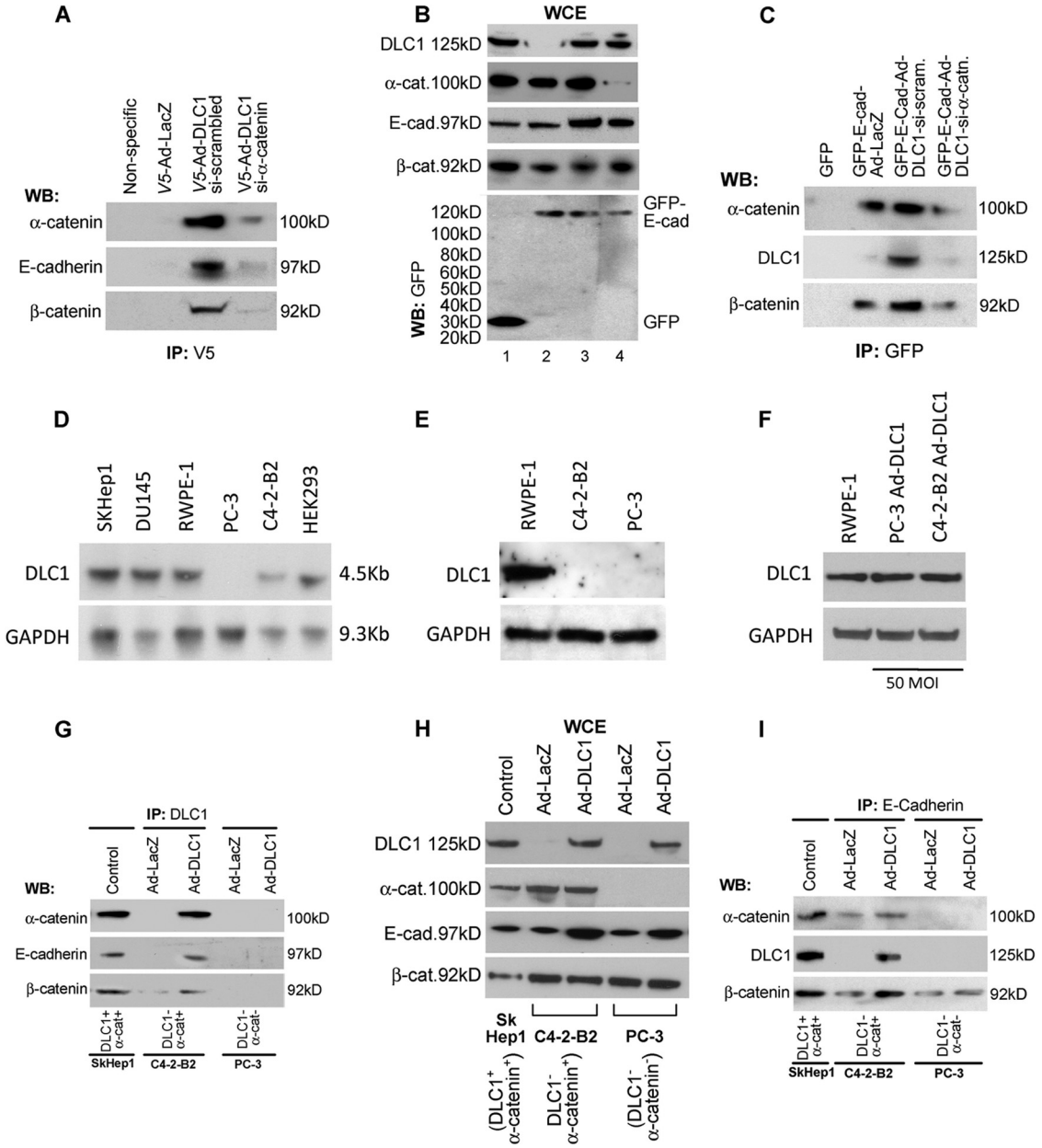

FIG 3 DLC1 interaction with the AJ complex proteins E-cadherin and β-catenin. (A) Immunoprecipitation with anti-V5 antibody of whole-cell extract of HEK 293 cells transduced and transfected with V5-tagged Ad-LacZ (lane 2), V5-tagged Ad-DLC1 plus "scrambled" siRNA (lane 3), and V5-tagged Ad-DLC1 plus α-catenin siRNA (lane 4) and Western blotted with anti-α-catenin, anti-E-cadherin, and anti-β-catenin antibodies, showing interaction of DLC1 with the AJ proteins E-cadherin and β-catenin through α-catenin. Lane 1 shows immunoprecipitation with a nonspecific antibody of Ad-DLC1-transduced extract. (B) Whole-cell extracts (WCE) of HEK293 cells, immunoprecipitated with nonspecific or anti-GFP antibody (lane 1) or with anti-GFP or anti-V5 antibody (lanes 2, 3, and 4). DLC1 and E-cadherin were tagged with V5 and GFP, respectively. (C) Immunoprecipitation with anti-GFP antibody of cells transfected with GFP (lane 1), GFP-E-cadherin plus Ad-LacZ (lane 2), GFP-E-cadherin plus Ad-DLC1 plus "scrambled" siRNA (lane 3), and GFP-E-cadherin plus Ad-DLC1 plus α-catenin siRNA (lane 4) and Western blotted with anti-α-catenin, anti-DLC1, and anti-β-catenin antibodies. (D) Southern blot analysis of DLC1 gene in cell lines used in the study. Genomic DNA was digested with EcoRI for detection of DLC1. Hybridization was done using DLC1 fragment using primers DLC1-1F and DLC1-1R. Glyceraldehyde-3-phosphate dehydrogenase (GAPDH) was used as a control. (E) Western blot of cell lysate of RWPE-1, C4-2-B2, and PC-3 cells with anti-DLC1 antibody, showing the DLC1 level. GAPDH was used as a control. (F) Western blot of cell lysate of RWPE-1 and Ad-DLC1-transduced (50 MOI) C4-2-B2 cells and PC-3 cells with anti-DLC1 antibody, showing the same level of DLC1 expression. GAPDH was used as a control. (G and H) Whole-cell extract from the SKHep1 (control), C4-2-B2, and PC-3 cell lines transduced with Ad-DLC1 or Ad-LacZ, immunoprecipitated with anti-DLC1 (left) or anti-E-cadherin antibodies (G), and Western blotted (H) with anti-DLC1, anti-α-catenin, anti-β-catenin, and anti-E-cadherin antibodies. (I) WCE of the SkHep1, C4-2-B2, and PC-3 cancer cell lines.

membrane (Fig. 5B). To more closely examine the nature of DLC1 and α-catenin interaction in the membrane assembly of these two proteins, we used three functionally different V5-tagged DLC1 variants [DLC(1 to 1091) (wild type), a GAP-deficient R718E variant, α-catenin-binding-incompetent DLC1(Δ340–435), and DLC1(435–1091)] in C4-2-B2 cells and analyzed the distribution of the two proteins. Only wild-type DLC1 accumulated α-catenin to the membrane and colocalized with it at cell-cell junctions; the

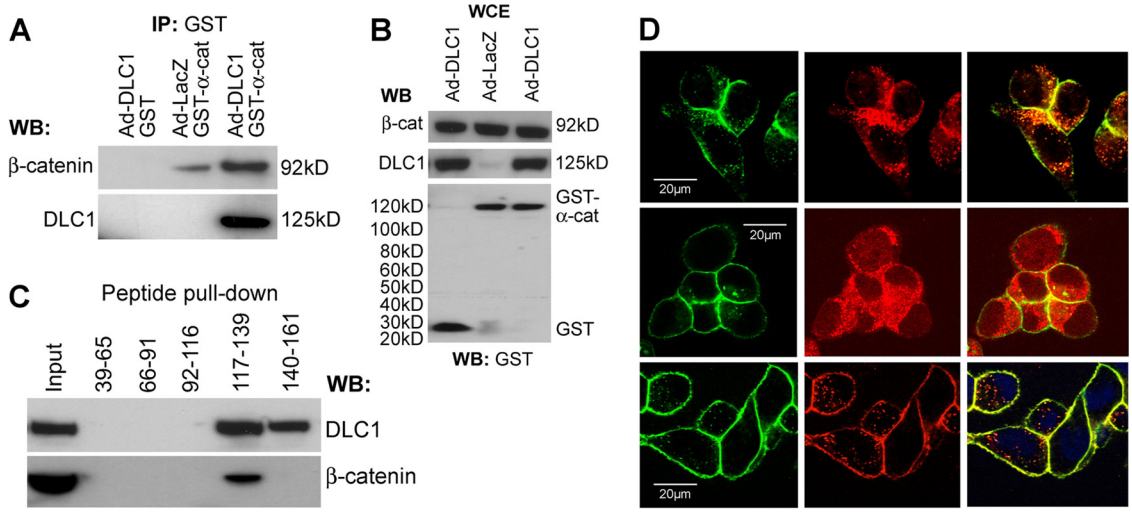

FIG 4 Interaction between α-catenin and β-catenin increases in the presence of DLC1. Anti-GST-antibody immunoprecipitation of extracts from HEK 293 cells transduced and transfected with Ad-DLC1 plus GST vector (lane 1), Ad-Lac Z plus GST–α-catenin (lane 2), and Ad-DLC1 plus GST-α-catenin (lane 3) and Western blotted with anti-β-catenin and anti-DLC1 antibodies. (B) WCE of GST-transfected and DLC1-transduced cells (lane 1), WCE of GST–α-catenin-transfected and LacZ-transduced cells (lane2), and WCE of GST–α-catenin-transfected and DLC1-transduced cells (lane 3). (C) Cell extract from HEK 293 cells transduced with V5-tagged Ad-DLC1 was used for streptavidin bead-based peptide pulldown of biotin-labeled peptides from the α-catenin aa 39 to 161 region and Western blotted with anti-V5 or anti-β-catenin antibody. (D) Colocalization of DLC1, α-catenin, E-cadherin, and β-catenin at cell-cell junctions in Ad-DLC1-transduced C4-2-B2 cells. Scale bar = 20 μm.

α-catenin-binding-incompetent variant, as expected, did not colocalize with α-catenin and remained in the cytoplasm, while the GAP-deficient yet α-catenin-binding-incompetent R718E variant colocalized with α-catenin, but both remained in the cytoplasm (Fig. 5C). Western blot analysis confirmed confocal immunofluorescence results (Fig. 5D); α-catenin accumulated in the membrane fraction only in the presence of full-length (wild-type) DLC1 but remained in a larger quantity in the cytosol when expressed with the GAP-deficient R718E variant or α-catenin-binding-incompetent DLC1(Δ340–435) or DLC1(435–1091). Alternatively, in order to prove this effect in normal cells, a fractionation experiment was done in the DLC1 knockdown prostate epithelial cell line RWPE-1 ($DLC1^+$/α-$catenin^+$). The result further confirmed that in the absence of DLC1, most of the α-catenin was present in the cytosol (Fig. 6A). An experiment with siRNA-suppressed expression of α-catenin in RWPE-1 cells showed that in the absence of α-catenin, DLC1 was localized mostly in the cytosol, whereas in the presence of α-catenin a good amount of DLC1 was contained in the membrane fraction (Fig. 6B). In order to prove that this mutual accumulation promotes α-catenin association with E-cadherin or the AJs, whole-cell extract of C4-2-B2 cells transfected with different DLC1 constructs was immunoprecipitated with E-cadherin antibody and tested for α-catenin. In the presence of full-length DLC1, there was a significant increase in E-cadherin-bound α-catenin, whereas the GAP-dead mutant and α-catenin-binding-incompetent DLC1 both failed to cause such an effect (Fig. 6C). These data show that interaction between DLC1 and α-catenin is critical for association of those two proteins with, and their accumulation at, the plasma membrane and that this process is fundamentally dependent on DLC1's GAP activity.

DLC1 affects mobility of E-cadherin and distribution of actin at AJs. A major characteristic of AJs is their ability to be continually created and disassembled in response to constant changes in the microenvironment (15), a feature instrumental for maintaining epithelial integrity and largely dependent on E-cadherin's mobility. Mature AJs result from binding of the E-cadherin–catenin complex to the element of the cytoskeleton and to several other molecules that may affect such mobility, one of which we hypothesize may be DLC1. To address the possibility that modulation of E-cadherin turnover is consequential to DLC1's interaction with AJs, we expressed a GFP–E-cadherin fusion construct in C4-2-B2 cells and showed that its behavior mimicked that of endogenous E-cadherin in both its intracellular distribution and its ability to interact with β-catenin (Fig. 7A and B). We then used fluorescence recovery after photobleaching (FRAP) to measure the mobility of GFP–E-cadherin fusion protein at the plasma membrane relative to the status of DLC1 and α-catenin. In the absence of DLC1, GFP–E-cadherin was recovered 31.4%, but in the presence of both DLC1 and α-catenin, the recovery reached 73.8% (Fig. 7D). The slope of the curve also indicates faster recovery of E-cadherin at cell-cell junctions, suggestive of its increased mobility in the presence of DLC1. To see if the absence of α-catenin modulates the dynamic of E-cadherin recovery at cell-cell junctions, we suppressed α-catenin expression by shRNA to approximately 15% (Fig. 7C). This resulted in a significant drop in E-cadherin recovery, from 73.8% to only 48.8%. Then we looked for the effect of the DLC1 GAP-dead mutant on E-cadherin recovery and learned that it reached only 40.3%, i.e., the level similar to the maximum of the DLC1-negative recovery curve, thus suggesting the role of DLC1 GAP activity in the process (Fig. 7D).

While E-cadherin mobility is instrumental in establishing AJs, their stabilization depends in large part on assembly of linear actin cables resulting from actin rearrangement in the presence of α-catenin at the membrane. To determine the role of DLC1–α-catenin interaction on actin cable formation and thus AJ stability, we examined DLC1- and α-catenin-transduced PC-3 cells after actin-specific phalloidin staining (Fig. 7E). The most pronounced

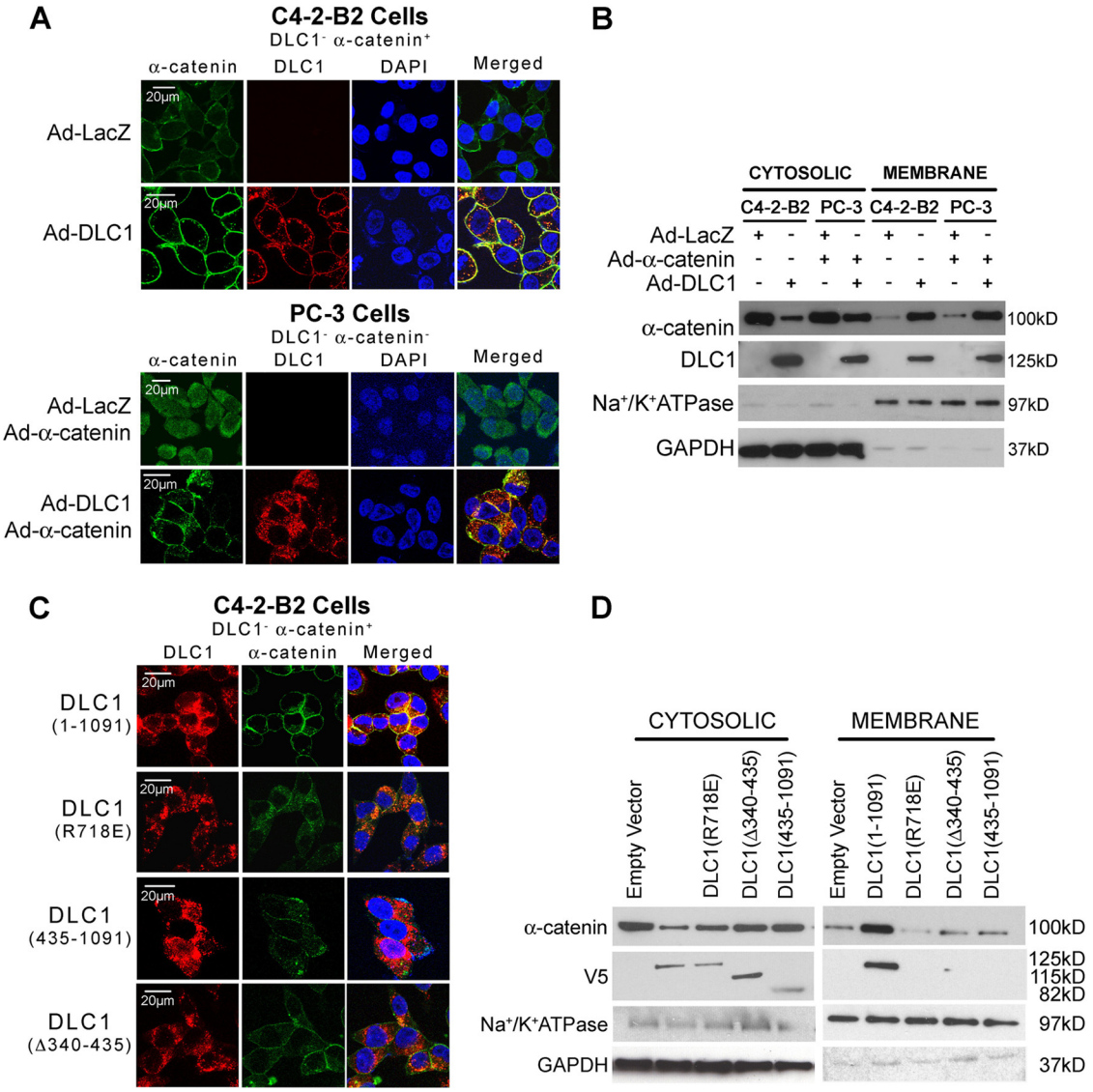

FIG 5 DLC1–α-catenin interaction accumulates α-catenin at the plasma membrane. (A) DLC1 and α-catenin immunofluorescence staining of C4-2-B2 and PC-3 cells transduced with Ad-DLC1, Ad-LacZ, or Ad-α-catenin. Scale bar = 20 μm. DAPI, 4′,6-diamidino-2-phenylindole. (B) Cytosolic and membrane fractions were Western blotted with anti-DLC1 and anti-α-catenin antibodies. (C) Immunofluorescence analysis of C4-2-B2 cells transfected with V5-tagged full-length DLC1, the DLC1 GAP mutant (R718E), DLC1(435–1091), and DLC1(Δ340–435) with anti-α-catenin and anti-V5-antibodies. Scale bar = 20 μm. (D) Western blot analysis of membrane and cytosolic fractions of the above-mentioned cells.

actin cables underlying AJs were observed in the presence of both DLC1 and α-catenin, suggesting that only together do they contribute to stabilization of AJs.

Effect of α-catenin on biological and oncosuppressive activity of DLC1. The ability of DLC1 to act as a RhoGAP and accelerate the conversion of active RhoGTP to inactive RhoGDP lies at the core of its proven tumor suppressor function (58). We sought to examine if and how α-catenin's interaction with DLC1 affects the latter's GAP activity.

C4-2-B2 cells express relatively high levels of both RhoGTP and α-catenin but lack endogenous DLC1 expression. We used full-length (wild type, amino acids 1 to 1091) DLC1, GAP-dead R718E DLC1, and α-catenin-binding-incompetent (Δ340–435) DLC1 constructs to evaluate the Rho response. We looked for Rho activity in membrane and cytosolic fractions (Fig. 8A). In cytosolic fractions, both the wild type and α-catenin-binding-incompetent DLC1 construct effectively decreased the amount of active Rho, due to their preserved GAP activity. GAP-dead DLC1 R718E understandably failed to do so regardless of α-catenin's availability (Fig. 8A). In the membrane fraction, though, the presence of α-catenin was instrumental for DLC1's suppression of active Rho. This result demonstrated that suppression of Rho activity at the membrane in cancer cells was due to DLC1 recruitment to the membrane through binding by α-catenin.

We further examined the effect of α-catenin on DLC1 oncosuppressive function. For this we selected metastatic PCA C4-2-B cells2 (DLC1$^-$/α-catenin$^+$) and PC-3 (DLC1$^-$/α-catenin$^-$). These cells were transduced and/or stably transfected in various combinations with Ad-LacZ, Ad-DLC1, and Ad-α-catenin/sh-α-catenin, and the resulting variants were examined for colony for-

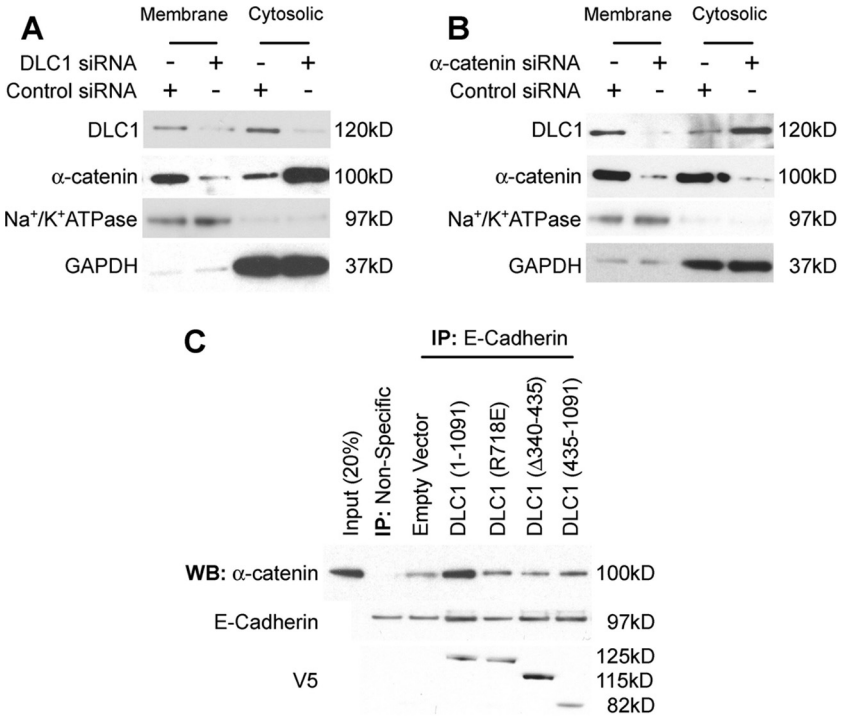

FIG 6 DLC1 increases α-catenin association with AJs. (A) DLC1-positive RWPE-1 cells were knocked down for anti-DLC1 using siDLC1; membrane and cytosolic fractions were Western blotted with anti-α-catenin and anti-DLC1 antibodies. (B) RWPE-1 cells were knocked down for α-catenin using si-α-catenin; membrane and cytosolic fractions were Western blotted for anti-DLC1 and anti-α-catenin antibody. (C) C4-2-B2 cells were transfected with V5-tagged full-length DLC1, the DLC1 GAP mutant (R718E), DLC1(435–1091), or DLC1(Δ340–435), and whole-cell extract was immunoprecipitated with anti-E-cadherin antibody and immunoblotted for anti-α-catenin antibody.

mation, invasion, and rate of apoptosis. Both C4-2-B2 and PC-3 DLC1-transduced cells formed fewer colonies and showed reduced invasiveness compared to findings for cells transduced with LacZ. Interestingly, the presence of α-catenin strongly potentiated a DLC1 inhibitory effect (Fig. 8B and C) on both colony formation (2.4-fold) and invasiveness (2.8-fold). These effects were validated on cells expressing the α-catenin-binding-incompetent DLC1 construct (Δ340–435). Cells containing the DLC1(R718E) GAP mutant formed colonies and showed invasiveness similar to that of the control (LacZ) cells, thus demonstrating that the DLC1 oncosuppressive function requires both the GAP function and the α-catenin/DLC1 binding. With regard to apoptosis, DLC1 transduction triggered an increase in apoptosis only in α-catenin-positive C4-2-B2 cells but not in α-catenin-negative PC-3 cells. Additional transduction of α-catenin in PC-3 cells, however, produced a significant increase in apoptosis. Similarly, suppression of α-catenin in C4-2-B2 cells by sh-α-catenin abrogated apoptosis in spite of the presence of DLC1 (Fig. 8D). These observations strongly suggest that interaction of DLC1 with α-catenin is required for maximum antioncogenic effects of DLC1.

DISCUSSION

In this study, we report that DLC1 binds α-catenin, a key component of complex molecular machinery responsible for cell-cell adhesion. This interaction results in an increased presence of both DLC1 and α-catenin at the plasma membrane, where they interact with the AJ complex proteins E-cadherin and β-catenin, modulate mobility of E-cadherin and distribution of actin, and consequently stabilize AJs. This interaction ultimately underlies the robust oncosuppressive action of DLC1.

The DLC1 gene was extensively investigated and repeatedly implicated as relevant to prostate cancer, in particular, by both our group and several other research teams around the world. In that respect, recurrent loss of DNA copy number and loss of heterozygosity in the genomic region harboring *DLC1* was reported in several studies of prostate neoplasia (2, 32, 33, 53), as was the downregulation or inactivation of *DLC1* by epigenetic mechanisms (18). Silencing of DLC1 in nonmalignant prostate cells promoted proangiogenic responses through vascular endothelial growth factor (VEGF) upregulation, an event considered highly significant in clinical assessment of prostate cancers (49). Conversely, restoration of DLC1 expression in prostate cancer cells resulted in inhibition of cell proliferation and tumorigenicity and in induction of apoptosis (17). Furthermore, a synergistic effect in suppressing tumorigenicity of metastatic prostate cancer cells was observed when DLC1 was aided by the histone deacetylase inhibitor SAHA (70). Last, in the most recent genome-wide array-based analysis of copy number alterations of prostate carcinomas, the highest frequency of copy number changes at the chromosomal location harboring *DLC1* and the evidences on epigenetic silencing of the gene lead the authors to concluded that DLC1 is, indeed, a factor in pathogenesis of prostate cancer (9). It is noteworthy that DLC1 has been conclusively shown to also suppress proliferation, invasion, and migration of cancer cells of nonprostate origin both *in vitro* and *in vivo* (13, 28, 30). Our finding that DLC1 interacts with α-catenin and through it with a cascade of adjoined

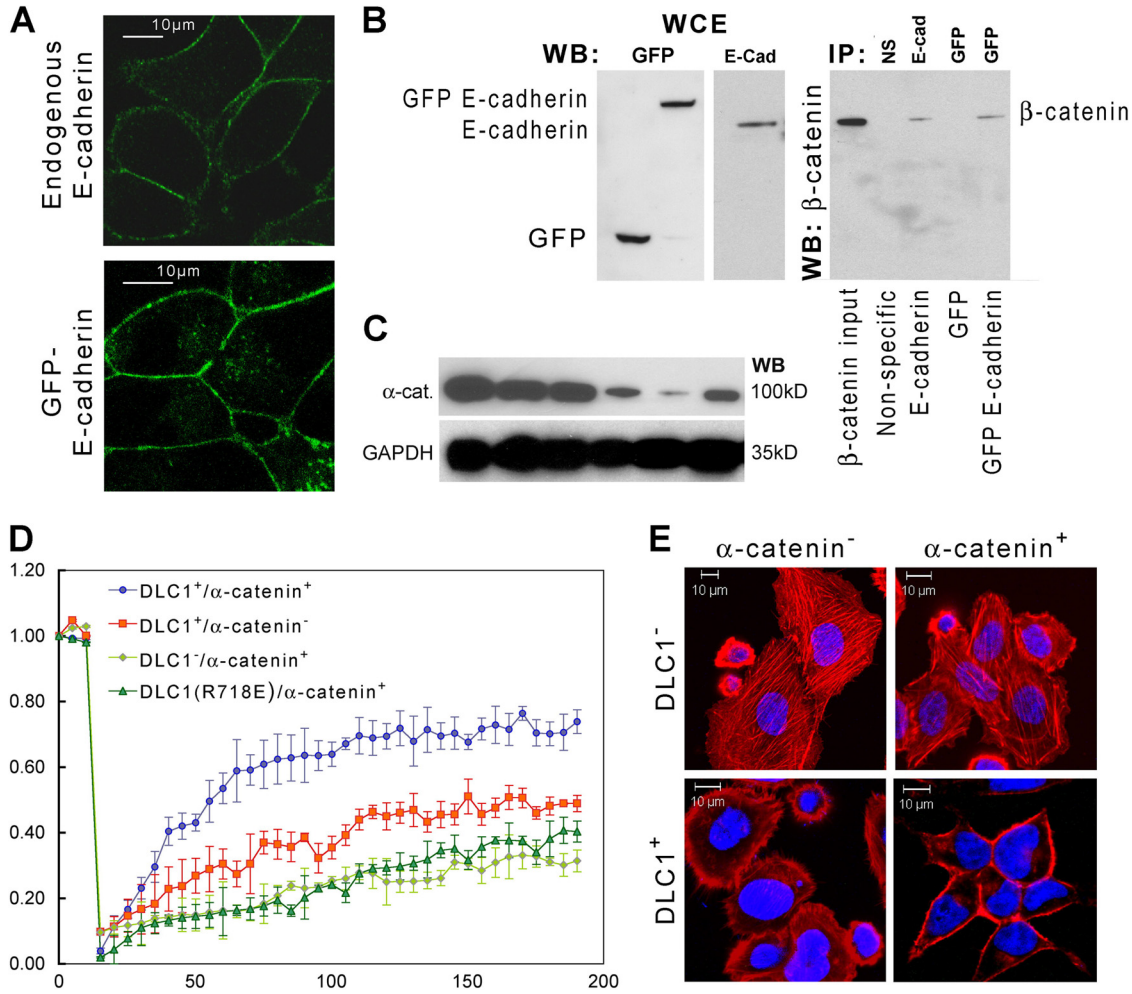

FIG 7 DLC1 affects the stability of AJs in the presence of α-catenin. (A) Immunofluorescence staining with anti-E-cadherin antibody. Scale bar = 10 μm. (B) Western blot analysis with anti-β-catenin antibodies of immunoprecipitates from lysates of C4-2-B2 cells with and without GFP-E-cadherin. (C) C4-2-B2 cells were transfected with four different Sure Silencing ShRNA plasmids (D1, D2, D3, and D4). RNA and protein analysis showed that clone D3 has maximum suppression of α-catenin (α-cat) expression. A plasmid containing a neomycin resistance gene was used as a negative control. (D) FRAP analysis of GFP–E-cadherin in C4-2-B2 cells transduced with Ad-LacZ, Ad-DLC1 alone, or Ad-DLC1 in combination with stable sh-α-catenin transfection and the DLC1 GAP mutant (R718E). (E) Phalloidin staining for the actin cytoskeleton in PC-3 cells transduced with either Ad-LacZ or Ad-DLC1 and/or Ad-α-catenin. Scale bar = 10 μm.

proteins, which together act as molecular stitches that maintain cell-cell adhesion, opens additional avenues for understanding DLC1's mechanisms of oncosuppression. Based on our finding that DLC1 stabilizes AJs, it is feasible to presume that by doing so it attenuates tumor-cell "shedding" and consequently their local and distant dissemination.

DLC1's binding partner α-catenin, on the other hand, is an important cytoplasmic molecular switch, which binds to the E-cadherin–β-catenin core of epithelial cell-cell junctions and regulates and binds the actin cytoskeletal structure (12). Absent or reduced α-catenin expression increases tumorigenic characteristics *in vitro* (37) and has been documented in esophageal, lung, stomach, pancreatic, and colorectal cancers (36, 38, 50). It has also been associated with metastasis (10, 11).

DLC1, a RhoGAP protein, binds with α-catenin through mutually recognized sites, which we identified as the N-terminal 340–435 amino acid segment in the DLC1 molecule and the 117–139 segment in α-catenin. Apparently, this same region in the α-catenin molecule (7, 24) has been found to enable interaction with β-catenin. The fact that DLC1 and β-catenin target the same amino acid range in α-catenin raises the question of whether they compete for or somehow share access to that spot. Our immunoprecipitation experiments showed unequivocally that DLC1 and β-catenin could simultaneously bind to α-catenin, whereas DLC1 cannot directly interact with β-catenin or E-cadherin (Fig. 3A and G). This ostensible paradox was explained by proving that DLC1 alternatively also interacts with the aa 140 to 161 segment of α-catenin, a site adjacent to the β-catenin binding site. Interestingly, the amount of β-catenin bound to α-catenin increases in the presence of DLC1, thus pointing to the possibility that β-catenin either shows higher affinity to α-catenin in the presence of DLC1 or has a preference for DLC1-bound α-catenin. Since β-catenin is a central molecule within the Wnt signaling cascade (34), modulation of the β-catenin–α-catenin interaction by DLC1 raises the question of potential association of DLC1 with the canonical Wnt pathway.

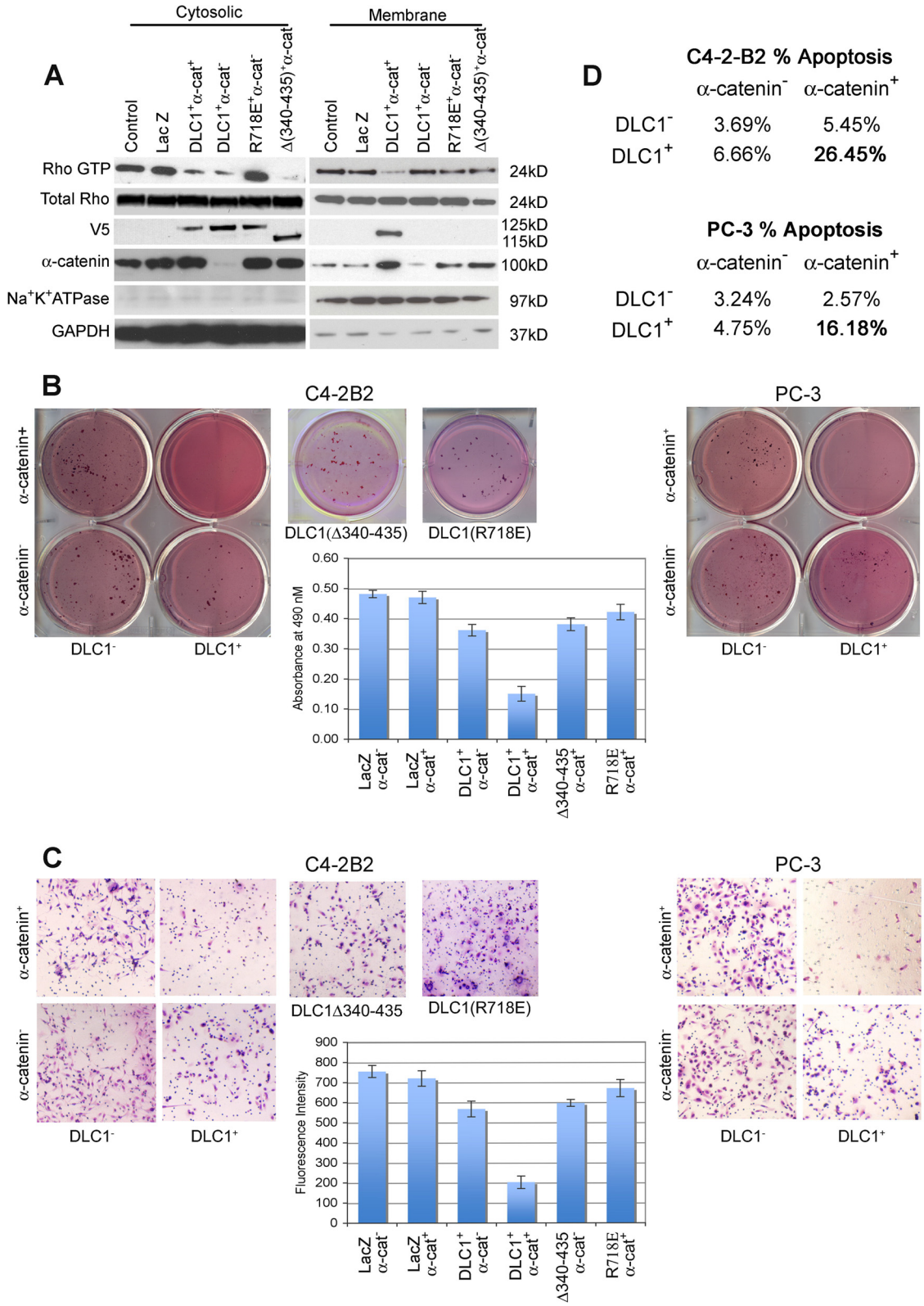

FIG 8 Effect of interaction of DLC1 with α-catenin on DLC1 oncosuppressive activity. (A) Active Rho (Rho GTP) level in C4-2-B2 cells. Cells were transduced with V5-tagged DLC1 or LacZ or stably transfected with V5-tagged Δ340–435 DLC1 and DLC1(R718E) in the presence and absence of α-catenin. Active Rho was assessed in membrane and cytosolic fractions by rhotekin assay, followed by Western blotting with anti-Rho antibody. Expression of total Rho, DLC1 (full length), DLC1(Δ340–435), DLC1(R718E), and α-catenin are shown. (B and C) The above-mentioned transduced/transfected C4-2-B2 cells and Ad-LacZ or Ad-DLC1 and Ad-α-catenin-transduced PC-3 cells were used for colony formation and invasion assays. For colony formation, cells were grown on 0.8% agar, and colony-forming efficiency was checked with staining; quantitation is shown in the graph in panel B. For the transwell invasion assay, cells were plated on a 24-well invasion chamber and stained for the invaded cells. Quantitative invasion was checked using fluoroBlok and is shown in the graph in panel C. (D) Effects of DLC1–α-catenin interaction on apoptosis were assessed by fluorescence-activated cell sorting (FACS) analysis of the above-described annexin V- and PI-stained C4-2-B2 and PC-3 cells. All values are means ± SD of three independent counts.

The interaction between α-catenin and DLC1 visibly affects the pattern of their intracellular distribution, because both of them become more apparent at the plasma membrane. Intracellular distribution of α-catenin appears to be relevant in malignant transformation. In PCA, for instance, abnormal α-catenin expression and cytoplasmic signal are statistically significantly associated with a higher T-category, high Gleason score, high mitotic rate, high S phase, and ultimately metastatic disease (1). Our results show that α-catenin accumulation at the membrane occurs only in the presence of full-length DLC1; it does not happen in the case where the DLC1 molecule carries an incapacitating mutation in its GAP domain; the GAP mutant binds α-catenin too, but the complex remains in the cytoplasm and never shows at the membrane. Accumulation of α-catenin at the membrane depends both on the intact DLC1's RhoGAP domain and on α-catenin–DLC1 binding. Interestingly, a mutant form of α-catenin, which lacks the extreme N terminus, also remains localized in the cytoplasm (7) because it fails to bind to β-catenin due to the deletion that eliminated the fragment between amino acids 46 and 149, which harbors a binding site for β-catenin. Although we are the first to report that α-catenin–DLC1 binding results in accumulation of both of them at the membrane, DLC1 is not the first RhoGAP to be associated with α-catenin; another member of the family, ARHGAP10, was also shown to recruit α-catenin and consequently control the actin cytoskeleton at cell-cell junctions and has a key role in *Listeria monocytogenes* invasion in epithelial cells (51). Also, α-catenin is not the only molecule whose relocation is aided by DLC1; it was shown earlier that cell migration is suppressed by DLC1-facilitated recruitment of EF1A1 to the cell periphery and ruffles via its SAM domain (67). Cytoplasmic localization of α-catenin appears as a fairly sensitive prognostic marker indicative of aggressive tumor behavior (4, 23), overall poor prognosis (35), and a low survival rate (42). Given that DLC1–α-catenin interaction modulates intracellular presentation of both molecules, the DLC1 pathway appears important for a better understanding of the disease.

The robust architecture of epithelial tissues and their stability depend on intercellular adhesion mediated by E-cadherin and supported by actin filaments. Our use of FRAP to address possible effects of DLC1–α-catenin interaction on the molecular dynamics of E-cadherin in cell-cell junctions and at the plasma membrane showed that in the presence of DLC1 and α-catenin, the recovery of bleached GFP–E-cadherin at cell-cell junctions was 73.8%, and the lateral mobility of E-cadherin molecules was significantly higher. Although E-cadherin mobility was shown to be different under *in vivo* and *in vitro* conditions (46), both the pattern and the slope of our FRAP results conform to the results described for *in vitro* conditions. In addition, our recovery curves were similar to those found earlier in CHO cells (52). The capacity of α-catenin to increase the lateral mobility of E-cadherin by modulating the dynamics of two actin populations has been also demonstrated in *Drosophila melanogaster* (8). Our result suggests that binding of DLC1 to α-catenin changes the nature of control that α-catenin exerts over the contractile actin network that affects lateral movement of E-cadherin.

Disturbed or week AJs have been found in highly malignant and metastatic cell lines, showing imbalances of the cell-cell adhesion proteins E-cadherin, α-catenin, and β-catenin (54). Rho GTPases are upregulated in various human cancers and are linked positively with progression of the disease (43). Overexpression of the Rho protein has been shown to disrupt AJs in colon carcinoma cells by actin-myosin contraction (44). DLC1 (a RhoGAP) colocalized with α-catenin both in the cytoplasm and at membranes, but their colocalization with β-catenin and E-cadherin occurred exclusively at AJs. Since lateral mobility of E-cadherin and thus stability of AJs appear to depend, at least in part, on specific conformation of the actin network, our observation that, in the presence of DLC1 and α-catenin, actin reorganizes around the cell periphery, as previously reported for nontransformed cells (3), comes in favor of the view that DLC1 has its role in stability of AJs. Accumulation of the DLC1–α-catenin complex at membranes certainly results in increased inhibition of Rho activity and subsequently in improved AJ stability. The data obtained with DLC1-knockout mice, showing that the loss of DLC1 is incompatible with normal embryonic development and survival (14), also points to DLC1's instrumental role in cell adhesion and in processes of establishing proper tissue architecture.

In conclusion, we have demonstrated for the first time that DLC1 and α-catenin interact and that their association leads to accumulation of both proteins at the plasma membrane, with a positive impact on the stability of AJs. We also showed that α-catenin-binding-incompetent DLC1 mutants featured attenuated oncosuppressive effects. Conversely, α-catenin-binding-incompetent wild-type DLC1 suppressed proliferation, invasion, and migration and triggered apoptosis, thus indicating that the strongest oncosuppressive effect results from DLC1 interaction with α-catenin. This interaction does not affect cytosolic Rho activity, whereas Rho activity in the cell membrane was suppressed due to the increased presence of DLC1, the effect instrumental for stabilization of AJs and an overall oncosuppressive function of DLC1.

ACKNOWLEDGMENTS

We have no conflicts of interest related to the manuscript to report.

This research was supported by the Intramural Research Program of the National Cancer Institute, National Institutes of Health.

REFERENCES

1. **Aaltomaa S, Lipponen P, Ala-Opas M, Eskelinen M, Kosma VM.** 1999. Alpha-catenin expression has prognostic value in local and locally advanced prostate cancer. Br. J. Cancer **80**:477–482.
2. **Arbieva ZH, et al.** 2000. High-resolution physical map and transcript identification of a prostate cancer deletion interval on 8p22. Genome Res. **10**:244–257.
3. **Ayollo DV, Zhitnyak IY, Vasiliev JM, Gloushankova NA.** 2009. Rearrangements of the actin cytoskeleton and E-cadherin-based adherens junctions caused by neoplasic transformation change cell-cell interactions. PLoS One **30**:e8027.
4. **Baloch ZW, Pasha T, LiVolsi VA.** 2001. Cytoplasmic accumulation of alpha-catenin in thyroid neoplasms. Head Neck **23**:573–578.
5. **Berx G, Van Roy F.** 2001. The E-cadherin/catenin complex: an important gatekeeper in breast cancer tumorigenesis and malignant progression. Breast Cancer Res. **3**:289–293.
6. **Bishop JM.** 1987. The molecular genetics of cancer. Science **235**:305–311.
7. **Bullions LC, Notterman DA, Chung LS, Levine AJ.** 1997. Expression of wild-type alpha-catenin protein in cells with a mutant alpha-catenin gene restores both growth regulation and tumor suppressor activities. Mol. Cell. Biol. **17**:4501–4508.
8. **Cavey M, Rauzi M, Lenne PF, Lecuit T.** 2008. A two-tiered mechanism for stabilization and immobilization of E-cadherin. Nature **453**:751–756.
9. **Cheng I, et al.** 2012. Copy number alterations in prostate tumors and disease aggressiveness. Genes Chromosomes Cancer **51**:66–76.
10. **Czyzewska J, Guzińska-Ustymowicz K, Ustymowicz MM, Pryczynicz A, Kemona A.** 2010. The expression of E-cadherin-catenin complex in patients with advanced gastric cancer: role in formation of metastasis. Folia Histochem. Cytobiol. **48**:37–45.

11. **Ding L, et al.** 2010. Genome remodelling in a basal-like breast cancer metastasis and xenograft. Nature **464**:999–1005.
12. **Drees F, Pokutta S, Yamada S, Nelson WJ, Weis WI.** 2005. Alpha-catenin is a molecular switch that binds E-cadherin-beta-catenin and regulates actin-filament assembly. Cell **123**:903–915.
13. **Durkin ME, et al.** 2007. DLC-1: a Rho GTPase-activating protein and tumour suppressor. J. Cell. Mol. Med. **11**:1185–1207.
14. **Durkin ME, et al.** 2005. DLC-1, a Rho GTPase-activating protein with tumor suppressor function, is essential for embryonic development. FEBS Lett. **579**:1191–1196.
15. **Giehl K, Menke A.** 2008. Microenvironmental regulation of E-cadherin-mediated adherens junctions. Front. Biosci. **13**:3975–3985.
16. **Goodison S, et al.** 2005. The RhoGAP protein DLC-1 functions as a metastasis suppressor in breast cancer cells. Cancer Res. **65**:6042–6053.
17. **Guan M, Tripathi V, Zhou X, Popescu NC.** 2008. Adenovirus-mediated restoration of expression of the tumor suppressor gene DLC1 inhibits the proliferation and tumorigenicity of aggressive, androgen-independent human prostate cancer cell lines: prospects for gene therapy. Cancer Gene Ther. **15**:371–381.
18. **Guan M, Zhou X, Soulitzis N, Spandidos DA, Popescu NC.** 2006. Aberrant methylation and deacetylation of deleted in liver cancer-1 gene in prostate cancer: potential clinical applications. Clin. Cancer Res. **12**:1412–1419.
19. **Hall A.** 2009. The cytoskeleton and cancer. Cancer Metastasis Rev. **28**:5–14.
20. **Hanahan D, Weinberg RA.** 2000. The hallmarks of cancer. Cell **100**: 57–70.
21. **Healy KD, et al.** 2008. DLC-1 suppresses non-small cell lung cancer growth and invasion by RhoGAP-dependent and independent mechanisms. Mol. Carcinog. **47**:326–337.
22. **Hirohashi S.** 1998. Inactivation of the E-cadherin-mediated cell adhesion system in human cancers. Am. J. Pathol. **153**:333–339.
23. **Hirvikoski P, et al.** 1998. Cytoplasmic accumulation of alpha-catenin is associated with aggressive features in laryngeal squamous-cell carcinoma. Int. J. Cancer **79**:546–550.
24. **Huber O, Krohn M, Kemler R.** 1997. A specific domain in alpha-catenin mediates binding to beta-catenin or plakoglobin. J. Cell Sci. **110**:1759–1765.
25. **Kadowaki T, et al.** 1994. E-cadherin and alpha-catenin expression in human esophageal cancer. Cancer Res. **54**:291–296.
26. **Kim TY, Vigil D, Der CJ, Juliano RL.** 2009. Role of DLC-1, a tumor suppressor protein with RhoGAP activity, in regulation of the cytoskeleton and cell motility. Cancer Metastasis Rev. **28**:77–83.
27. **Kim TY, et al.** 2008. Effects of structure of Rho GTPase-activating protein DLC-1 on cell morphology and migration. J. Biol. Chem. **283**:32762–32770.
28. **Ko FC, et al.** 2010. Akt phosphorylation of deleted in liver cancer 1 abrogates its suppression of liver cancer tumorigenesis and metastasis. Gastroenterology **139**:1397–1407.
29. **Lahoz A, Hall A.** 2008. DLC1: a significant GAP in the cancer genome. Genes Dev. **22**:1724–1730.
30. **Liao YC, Lo SH.** 2008. Deleted in liver cancer-1 (DLC-1): a tumor suppressor not just for liver. Int. J. Biochem. Cell Biol. **40**:843–847.
31. **Liao Y-C, Si L, DeVere White RW, Lo SH.** 2007. The phosphotyrosine-independent interaction of DLC-1 and the SH2 domain of cten regulates focal adhesion localization and growth suppression activity of DLC-1. J. Cell Biol. **176**:43–49.
32. **Macoska JA, et al.** 1995. Evidence for three tumor suppressor gene loci on chromosome 8p in human prostate cancer. Cancer Res. **55**:5390–5395.
33. **Matsuyama H, et al.** 2001. Deletions on chromosome 8p22 may predict disease progression as well as pathological staging in prostate cancer. Clin. Cancer Res. **7**:3139–3143.
34. **Moon RT, Bowerman B, Boutros M, Perrimon N.** 2002. The promise and perils of Wnt signaling through beta-catenin. Science **296**:1644–1646.
35. **Nakopoulou L, et al.** 2002. Abnormal alpha-catenin expression in invasive breast cancer correlates with poor patient survival. Histopathology **40**:536–546.
36. **Pirinen RT, Hirvikoski P, Johansson RT, Hollmén S, Kosma VM.** 2001. Reduced expression of alpha-catenin, beta-catenin, and gamma-catenin is associated with high cell proliferative activity and poor differentiation in non-small cell lung cancer. J. Clin. Pathol. **54**:391–395.
37. **Plumb CL, et al.** 2009. Modulation of the tumor suppressor protein alpha-catenin by ischemic microenvironment. Am. J. Pathol. **175**:1662–1674.
38. **Pryczynicz A, Guzińska-Ustymowicz K, Kemona A, Czyzewska J.** 2010. Expression of the E-cadherin-catenin complex in patients with pancreatic ductal adenocarcinoma. Folia Histochem. Cytobiol. **48**:128–133.
39. **Qian X, et al.** 2007. Oncogenic inhibition by a deleted in liver cancer gene requires cooperation between tensin binding and Rho-specific GTPase-activating protein activities. Proc. Natl. Acad. Sci. U. S. A. **104**:9012–9017.
40. **Richmond PJ, Karayiannakis AJ, Nagafuchi A, Kaisary AV, Pignatelli M.** 1997. Aberrant E-cadherin and alpha-catenin expression in prostate cancer: correlation with patient survival. Cancer Res. **57**:3189–3193.
41. **Rimm DL, Koslov ER, Kebriaei P, Cianci CD, Morrow JS.** 1995. Alpha 1(E)-catenin is an actin-binding and -bundling protein mediating the attachment of F-actin to the membrane adhesion complex. Proc. Natl. Acad. Sci. U. S. A. **92**:8813–8817.
42. **Ropponen KM, Eskelinen MJ, Lipponen PK, Alhava EM, Kosma VM.** 1999. Reduced expression of alpha catenin is associated with poor prognosis in colorectal carcinoma. J. Clin. Pathol. **52**:10–16.
43. **Sahai E, Marshall CJ.** 2002. RHO-GTPases and cancer. Nat. Rev. Cancer **2**:133–142.
44. **Sahai E, Marshall CJ.** 2002. ROCK and Dia have opposing effects on adherens junctions downstream of Rho. Nat. Cell Biol. **4**:408–415.
45. **Scholz RP, et al.** 2009. DLC1 interacts with 14-3-3 proteins to inhibit RhoGAP activity and block nucleocytoplasmic shuttling. J. Cell Sci. **122**: 92–102.
46. **Serrels A, et al.** 2009. Real-time study of E-cadherin and membrane dynamics in living animals: implications for disease modeling and drug development. Cancer Res. **69**:2714–2719.
47. **Setoyama T, et al.** 2007. Alpha-catenin is a significant prognostic factor than E-cadherin in esophageal squamous cell carcinoma. J. Surg. Oncol. **95**:148–155.
48. **Shih YP, Yoshikazu T, Hao LS.** 2012. Silencing of DLC1 upregulates PAI-1 expression and reduces migration in normal prostate cells. Mol. Cancer Res. **10**:34–39.
49. **Shih YP, Liao YC, Lin Y, Lo SH.** 2010. DLC1 negatively regulates angiogenesis in a paracrine fashion. Cancer Res. **70**:8270–8275.
50. **Shiozaki H, et al.** 1994. Immunohistochemical detection of alpha-catenin expression in human cancers. Am. J. Pathol. **144**:667–674.
51. **Sousa S, et al.** 2005. ARHGAP10 is necessary for alpha-catenin recruitment at adherens junctions and for Listeria invasion. Nat. Cell Biol. **7**:954–960.
52. **Stehbens SJ, et al.** 2006. Dynamic microtubules regulate the local concentration of E-cadherin at cell-cell contacts. J. Cell Sci. **119**:1801–1811.
53. **Struski S, Doco-Fenzy M, Cornillet-Lefebvre P.** 2002. Compilation of published comparative genomic hybridization studies. Cancer Genet. Cytogenet. **135**:63–90.
54. **Thiery JP.** 2002. Epithelial-mesenchymal transitions in tumour progression. Nat. Rev. Cancer **2**:442–454.
55. **Ullmannova-Benson V, et al.** 2009. DLC1 tumor suppressor gene inhibits migration and invasion of multiple myeloma cells through RhoA GTPase pathway. Leukemia **23**:383–390.
56. **Vasioukhin V, Bauer C, Degenstein L, Wise B, Fuchs E.** 2001. Hyperproliferation and defects in epithelial polarity upon conditional ablation of alpha-catenin in skin. Cell **104**:605–617.
57. **Vermeulen SJ, et al.** 1995. Transition from the noninvasive to the invasive phenotype and loss of alpha-catenin in human colon cancer cells. Cancer Res. **55**:4722–4728.
58. **Vigil D, Cherfils J, Rossman Kl, Der CJ.** 2010. Ras superfamily GEFs and GAPs: validated and tractable targets for cancer therapy? Nat. Rev. Cancer **12**:842–857.
59. **Wong CM, et al.** 2005. Rho GTPase-activating protein deleted in liver cancer suppresses cell proliferation and invasion in hepatocellular carcinoma. Cancer Res. **65**:8861–8868.
60. **Xue W, et al.** 2008. DLC1 is a chromosome 8p tumor suppressor whose loss promotes hepatocellular carcinoma. Genes Dev. **22**:1439–1444.
61. **Yam JW, Ko FC, Chan CY, Jin DY, Ng IO.** 2006. Interaction of deleted in liver cancer 1 with tensin2 in caveolae and implications in tumor suppression. Cancer Res. **66**:8367–8372.
62. **Yang X, Popescu NC, Zimonjic DB.** 2011. DLC1 interaction with S100A10 mediates inhibition of in vitro cell invasion and tumorigenicity of lung cancer cells through a RhoGAP-independent mechanism. Cancer Res. **71**:2916–2925.
63. **Yang XY, et al.** 2009. p120Ras-GAP binds the DLC1 Rho-GAP tumor suppressor protein and inhibits its RhoA GTPase and growth-suppressing activities. Oncogene **28**:1401–1409.
64. **Yuan BZ, Jefferson AM, Millecchia L, Popescu NC, Reynolds SH.** 2007.

Morphological changes and nuclear translocation of DLC1 tumor suppressor protein precede apoptosis in human non-small cell lung carcinoma cells. Exp. Cell Res. **313**:3868–3880.
65. **Yuan BZ, et al.** 2004. DLC-1 operates as a tumor suppressor gene in human non-small cell lung carcinomas. Oncogene **23**:405–411.
66. **Yuan BZ, et al.** 1998. Cloning, characterization, and chromosomal localization of a gene frequently deleted in human liver cancer (DLC-1) homologous to rat RhoGAP. Cancer Res. **58**:2196–2199.
67. **Zhong D, et al.** 2009. The SAM domain of the RhoGAP DLC1 binds EF1A1 to regulate cell migration. J. Cell Sci. **122**:414–424.
68. **Zhou X, et al.** 2008. DLC1 suppresses distant dissemination of human hepatocellular carcinoma cells in nude mice through reduction of RhoA GTPase activity, actin cytoskeletal disruption and down regulation of genes involved in metastasis. Int. J. Oncol. **32**:1258–1291.
69. **Zhou X, Thorgeirsson SS, Popescu NC.** 2004. Restoration of DLC-1 gene expression induces apoptosis and inhibits both cell growth and tumorigenicity in human hepatocellular carcinoma cells. Oncogene **23**:1308–1313.
70. **Zhou X, Yang X-Y, Popescu NC.** 2010. Synergistic antineoplastic effect of DLC1 tumor suppressor protein and histone deacetylase inhibitor, suberoylanilide hydroxamic acid (SAHA), on prostate and liver cancer cells: perspectives for therapeutics. Int. J. Oncol. **36**:999–1005.